Quantum Simulation of Interacting Fermion Lattice Models in Trapped Ions

J. Casanova,[1] A. Mezzacapo,[1] L. Lamata,[1] and E. Solano[1,2]

[1]*Departamento de Química Física, Universidad del País Vasco UPV/EHU, Apdo. 644, 48080 Bilbao, Spain*
[2]*IKERBASQUE, Basque Foundation for Science, Alameda Urquijo 36, 48011 Bilbao, Spain*
(Received 28 November 2011; published 10 May 2012)

We propose a method of simulating efficiently many-body interacting fermion lattice models in trapped ions, including highly nonlinear interactions in arbitrary spatial dimensions and for arbitrarily distant couplings. We map products of fermionic operators onto nonlocal spin operators and decompose the resulting dynamics in efficient steps with Trotter methods, yielding an overall protocol that employs only polynomial resources. The proposed scheme can be relevant in a variety of fields such as condensed-matter or high-energy physics, where quantum simulations may solve problems intractable for classical computers.

Quantum simulations promise to revolutionize computing technologies and scientific research by allowing us to solve problems that are otherwise intractable with classical computers [1,2]. Several physical systems have been proposed in a quantum simulator: spin models [3–6], quantum phase transitions [7], quantum chemistry [8], anyonic statistics [9], many-body systems with Rydberg atoms [10], and relativistic systems [11–18]. Trapped ions offer one of the most promising platforms for quantum simulators [19], due to their high controllability, efficient initialization, and measurement [20]. In the near future, experiments in quantum simulations should be able to solve problems intractable for classical computers, turning this technology into a remarkable tool for scientists and engineers.

The numerical simulation of fermionic systems is, in general, a hard problem due to the huge increase of the Hilbert space dimension with the number of modes [1,21]. Using customized numerical methods such as quantum Monte Carlo calculations is not always possible due to the well-known sign problem [22,23]. Quantum simulations appear as a tool that will allow us to compute the time evolution of free and interacting fermion lattice theories with minimal experimental resources. This will be helpful in performing a wide range of condensed-matter calculations, including those related to many-body interactions such as the Kondo [24], Fermi-Hubbard [25], or Fröhlich [26] Hamiltonians. Furthermore, quantum simulations will allow us to reproduce the complete dynamics of these systems, avoiding mean field approximations such as the Hartree-Fock approximation to simplify nonlinear interactions [27].

In this Letter, we propose a method of realizing the quantum simulation of many-body fermionic lattice models for N fermionic modes in trapped ions. Our method can be described in three steps. Firstly, we map the set of N fermionic modes, via the Jordan-Wigner transformation [28], to a set of N nonlocal spin operators. The second step consists in decomposing the total unitary evolution via

Trotter expansion [2,29,30] in terms of a product of exponentials associated with each nonlocal spin operator appearing in the Hamiltonian. Finally, we implement each of these exponentials in polynomial time on a set of N two-level trapped ions with a reduced number of laser pulses [31,32]. These three steps yield an efficient protocol that employs only polynomial resources. Our method can simulate highly nonlinear and long-range interactions in arbitrary spatial dimensions, applying the Jordan-Wigner transformation without the usual restriction of a reduced number of neighbors, and without the need of auxiliary virtual Majorana fermions [33]. This is due to the fact that the dynamics associated with the nonlocal spin operators, containing a large number of Pauli matrices, can still be efficiently implemented. The proposed protocol opens the possibility to simulate a wide range of interesting condensed-matter and high-energy physics fermionic systems for a large number of particles. This includes the calculation of time evolutions and ground state computations, e.g., through adiabatic protocols [34]. For a number of particles above ~30, which is foreseeable in the near future, one could already simulate fermionic systems that are intractable for classical computers.

We consider the quantum simulation of the dynamics associated with the general Hamiltonian

$$H = \sum_{n=2}^{\alpha} \left[\sum_{i_1...i_n=1}^{N} g_{i_1...i_n} c_{i_1} \cdots c_{i_n} + \text{H.c.} \right], \quad (1)$$

where c_{i_k} has to be chosen as one of the fermionic operators b_{i_k}, $b_{i_k}^{\dagger}$, that obey the anticommutation rule $\{b_{i_k}, b_{i_{k'}}^{\dagger}\} = \delta_{i_k,i_{k'}}$, N is the number of fermionic modes, and α is the highest order of the many-body interaction.

Our protocol consists of three steps, gathering techniques that have not been previously considered for quantum simulators of fermionic lattice models [35].

(i) *Jordan-Wigner mapping.*—This technique establishes a correspondence between a set of fermionic operators and

a set of spin operators, transforming a local Hamiltonian of fermions onto a nonlocal Hamiltonian of spins. Only in one spatial dimension, and for couplings extended to a reduced number of neighbors, the correspondence is from a local model to a similar one [28]. The operators b_{i_k}, $b_{i_k}^\dagger$ can always be mapped to products of Pauli matrices, i.e., non-local spin operators, using the Jordan-Wigner transformation $b_k^\dagger = I_N \otimes I_{N-1} \otimes \ldots \otimes \sigma_k^+ \otimes \sigma_{k-1}^z \otimes \ldots \otimes \sigma_1^z$, and $b_k = (b_k^\dagger)^\dagger$.

(ii) *Trotter decomposition of the total Hamiltonian.*— Our second step consists in using standard Trotter techniques to decompose the total evolution operator in terms of a product of evolution operators associated to each nonlocal spin operator. We prove below that these evolution operators can be implemented efficiently.

(iii) *Implementation of nonlocal spin operators in trapped ions.*—The exponentials of each nonlocal spin operator are efficiently implementable, given that their exponents consist of tensor products of k Pauli matrices. Each of these exponentials can be implemented, for arbitrary k and up to local rotations, with a Mølmer-Sørensen gate upon k ions, one local gate upon one of the ions, and the inverse Mølmer-Sørensen gate [31]. This step can be summarized as

$$\mathcal{U} = \mathcal{U}_{\text{MS}}(-\pi/2, 0)\,\mathcal{U}_{\sigma_z}(\phi)\,\mathcal{U}_{\text{MS}}(\pi/2, 0)$$
$$= \exp[i\phi\sigma_1^z \otimes \sigma_2^x \otimes \sigma_3^x \otimes \cdots \otimes \sigma_k^x], \quad (2)$$

where $\mathcal{U}_{\text{MS}}(\theta, \phi) = \exp[-i\theta(\cos\phi S_x + \sin\phi S_y)^2/4]$, $S_{x,y} = \sum_{i=1}^k \sigma_i^{x,y}$, and $\mathcal{U}_{\sigma_z}(\phi) = \exp(i\phi'\sigma_1^z)$ for odd k, where $\phi' = \phi$ for $k = 4n + 1$, and $\phi' = -\phi$ for $k = 4n - 1$, with positive integer n. For even k, $\mathcal{U}_{\sigma_z}(\phi)$ would be substituted by $\mathcal{U}_{\sigma_y}(\phi) = \exp(i\phi'\sigma_1^y)$, where $\phi' = \phi$ for $k = 4n$, and $\phi' = -\phi$ for $k = 4n - 2$, with positive integer n. In order to obtain directly a coupling composed of σ^y matrices times a σ^z, one may apply a similar approach with different Mølmer-Sørensen gates according to

$$\mathcal{U} = \mathcal{U}_{\text{MS}}(-\pi/2, \pi/2)\,\mathcal{U}_\sigma(\phi)\,\mathcal{U}_{\text{MS}}(\pi/2, \pi/2)$$
$$= \exp[i\phi\sigma_1^z \otimes \sigma_2^y \otimes \sigma_3^y \otimes \cdots \otimes \sigma_k^y], \quad (3)$$

where the local $\mathcal{U}_\sigma(\phi)$ gate is $\exp(i\phi'\sigma_1^z)$ for odd k, where $\phi' = \phi$ for $k = 4n + 1$, and $\phi' = -\phi$ for $k = 4n - 1$, with positive integer n. For even k, the local gate is $\exp(i\phi'\sigma_1^x)$ where $\phi' = \phi$ for $k = 4n - 2$, and $\phi' = -\phi$ for $k = 4n$, with positive integer n. Note that local rotations acting on each ion give rise to any tensor product of Pauli matrices $\sigma_k^{x,y,z}$. The coupling constant in each nonlocal spin term of the simulated Hamiltonian (1) will be related to ϕ through $\phi = -gt$, where g is a generic coupling strength and t is the corresponding gate time (for details, see [35]).

The three steps of our protocol amount to an efficient method for simulating fermionic models with long-range couplings in arbitrary dimensions with trapped ions.

Note that for bounded Hamiltonians, the Trotter expansion associated with the exponential of the polynomial sum of efficiently implementable nonlocal terms is also efficient [2,29,30]; i.e., it only requires polynomial resources [35]. This includes most fermionic models in condensed-matter and high-energy physics, some of which we consider below.

Kondo model.—The long debated Kondo Hamiltonian provides a variety of interesting features in different systems, as the minimum in the resistivity at low temperatures [36]. With the proposed method, we can simulate Kondo Hamiltonians [24], modelling the interaction of a Fermi sea of electrons with several magnetic impurities at positions R_j,

$$H = \sum_{p\sigma}\epsilon_p b_{p\sigma}^\dagger b_{p\sigma} - J\sum_{pp'j} e^{iR_j \cdot (p - p')}[(b_{p\uparrow}^\dagger b_{p'\uparrow} - b_{p\downarrow}^\dagger b_{p'\downarrow})\sigma_j^z$$
$$+ b_{p\uparrow}^\dagger b_{p'\downarrow}\sigma_j^- + b_{p\downarrow}^\dagger b_{p'\uparrow}\sigma_j^+]. \quad (4)$$

Here, $\sigma = \uparrow, \downarrow$ is the spin of the electron, $b_{p,p'\uparrow}(b_{p,p'\uparrow}^\dagger)$ is the annihilation (creation) operator for an electron with respective momentum p or p' and spin up, $\sigma_j^+(\sigma_j^-)$ is the impurity raising (lowering) spin operator, ϵ_p is the energy of the kinetic electronic Hamiltonian, and J is the electron-impurity coupling. Notice that, e.g., the operators $b_{p\uparrow}^\dagger b_{p'\downarrow}\sigma_j^-$ can now be mapped to a sum of products of Pauli matrices, leading to an efficient implementation.

Fermi-Hubbard model.—The Fermi-Hubbard Hamiltonian [25] takes into account a range of effects in condensed-matter physics, as the Mott transition, and is also believed to be relevant in high-T_c superconductivity. It takes the form

$$H = w\sum_{\delta i\sigma} b_{i\sigma}^\dagger b_{i+\delta\sigma} + U\sum_j b_{j\uparrow}^\dagger b_{j\uparrow} b_{j\downarrow}^\dagger b_{j\downarrow}, \quad (5)$$

where the first fermionic operator subindex refers to the lattice site and the second to the spin, w is the hopping energy, U is the on site Coulomb repulsion and one usually makes the tight-binding approximation $\delta = \pm 1$. Notice that our method is general and extends the hopping terms to arbitrarily distant pairs of electrons. The last term contains the product of four fermionic operators, allowing for efficient implementation.

We could as well implement the coupling of arbitrary products of fermionic operators [similar to Eq. (1)] to the linear sum of bosonic operators,

$$H = \sum_{n=2}^\alpha \left[\sum_{i_1 \ldots i_n = 1}^N g_{i_1 \cdots i_n} c_{i_1} \cdots c_{i_n} \sum_j g_j(a_j + a_j^\dagger) + \text{H.c.} \right]. \quad (6)$$

The bosonic operators a_j can be implemented with the vibrational modes of the ion chain. One would now

consider the same gate sequence as in Eq. (2) but replacing $\mathcal{U}_{\sigma_z}(\phi) = \exp(i\phi'\sigma^z)$ with $\mathcal{U}_{\sigma_z,a}(\phi) = \exp[i\phi'\sigma^z \sum_j g_j(a_j + a_j^\dagger)]$. The latter can be implemented by using red and blue sideband interactions for each of the a_j modes in the context of standard trapped-ion technology [37].

Fröhlich model.—The Fröhlich Hamiltonian [26] models the interaction of electrons with phonons,

$$H = \sum_p \frac{p^2}{2m} b_p^\dagger b_p + \omega_0 \sum_q a_q^\dagger a_q$$
$$+ \sum_{qp} M(q) b_{p+q}^\dagger b_p (a_q + a_{-q}^\dagger), \qquad (7)$$

with $M(q)$ being the electron-phonon coupling. Here, b_p is the electron annihilation operator that destroys an electron with momentum p, a_q is the phonon annihilation operator with momentum q, ω_0 is the phonon frequency, and m is the electron mass. The last term contains the product $b_{p+q}^\dagger b_p (a_q + a_{-q}^\dagger)$, whose dynamics can be implemented with our technique above according to Eq. (6). We can simulate this kind of Hamiltonian in order to recover the polaron physics, a critical open issue for the deep understanding of correlated electrons in solids [38].

One of the main appeals of our method is that the efficient encoding of fermionic models in a lattice with arbitrarily long-range couplings is feasible. This also means that we can apply the Jordan-Wigner transformation for two and three spatial dimensions, not just for one, without employing additional virtual Majorana fermions [33]. All this is due to the fact that the fermionic operators are encoded in nonlocal spin operators whose dynamics are efficiently implementable. Thus, the mapped spin Hamiltonians are highly nonlocal but their evolution is efficiently realizable. In order to show this, we plot in Fig. 1 the mapping of a solid-state 3D fermionic system onto an ion string. As opposite to the nearest-neighbor tunneling coupling between fermions 1 and 2, which is local, the couplings between 1 and 4, and between 1 and 10, are nonlocal due to the Jordan-Wigner transformation [see Fig. 1(a)]. Nevertheless, we can implement them in an efficient way. In Fig. 1(b), we show the implementation of the tunneling coupling $b_1^\dagger b_{10} + b_{10}^\dagger b_1 = \sigma_1^x \otimes \sigma_2^z \otimes \sigma_3^z \otimes \ldots \otimes \sigma_9^z \otimes \sigma_{10}^x + \sigma_1^y \otimes \sigma_2^z \otimes \sigma_3^z \otimes \ldots \otimes \sigma_9^z \otimes \sigma_{10}^y$ in trapped ions. This highly nonlocal coupling is a global unitary of $2^{10} \times 2^{10}$ dimensions. In the general case, it would require a number of elementary gates of $2^{20} \simeq 10^6$ [2]. With our method, the number of gates can be as small as 10 per Trotter step, consisting of Mølmer-Sørensen gates (dark blue and green, second, fourth, seventh and ninth gates starting from the left), local $\exp(i\phi'\sigma_2^y)$ gates (red, third and eighth gates starting from the left), $\exp[\pm i(\pi/4)\sum_i \sigma_i^y]$ (yellow, sixth and tenth gates starting from the left), and $\exp[\pm i(\pi/4)\sum_i \sigma_i^x]$ (cyan, first and fifth gates starting from the left) gates [see Fig. 1(b)] [35].
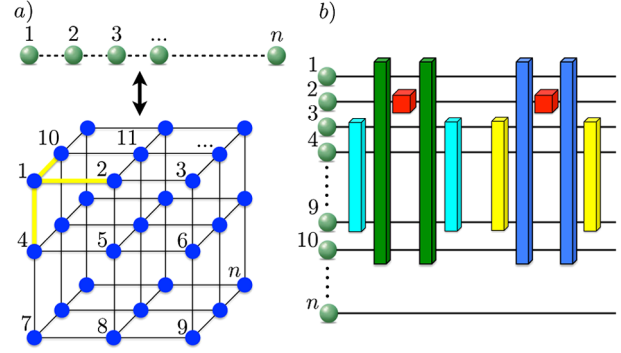

FIG. 1 (color online). (a) Mapping of a fermionic Hamiltonian onto an ion string. The couplings between fermions 1 and 4 (respectively, 1 and 10) are nonlocal when applying the Jordan-Wigner transformation. (b) Efficient mapping of the tunneling coupling $b_1^\dagger b_{10} + b_{10}^\dagger b_1$ in trapped ions. This highly nonlocal coupling can be implemented with Mølmer-Sørensen gates (dark blue and green, second, fourth, seventh and ninth gates starting from the left), local $\exp(i\phi'\sigma_2^y)$ gates (red, third and eighth gates starting from the left), $\exp[\pm i(\pi/4)\sum_i \sigma_i^y]$ (yellow, sixth and tenth gates starting from the left), and $\exp[\pm i(\pi/4)\sum_i \sigma_i^x]$ (cyan, first and fifth gates starting from the left) gates.

Numerical simulations.—In order to compare the efficiency of the Trotter decomposition with the exact case, we have realized numerical simulations of the Fermi-Hubbard Hamiltonian, Eq. (5), for different levels of Trotter expansion and for the exact diagonalization case. We have considered the case of three lattice sites, with six modes (two spins per site), to be simulated with six two-level trapped ions. The resulting Hamiltonian is

$$H = w(b_{1\uparrow}^\dagger b_{2\uparrow} + b_{1\downarrow}^\dagger b_{2\downarrow} + b_{2\uparrow}^\dagger b_{3\uparrow} + b_{2\downarrow}^\dagger b_{3\downarrow} + \text{H.c.})$$
$$+ U(b_{1\uparrow}^\dagger b_{1\uparrow} b_{1\downarrow}^\dagger b_{1\downarrow} + b_{2\uparrow}^\dagger b_{2\uparrow} b_{2\downarrow}^\dagger b_{2\downarrow} + b_{3\uparrow}^\dagger b_{3\uparrow} b_{3\downarrow}^\dagger b_{3\downarrow}). \quad (8)$$

Notice that the number of terms to be implemented scales linearly with the number of modes, $5N/2 - 4$ (11 in this case, for $N = 6$). At the same time, the nonlocal gates upon several ions are efficiently implementable with few lasers, such that the number of gates in each term of the Hamiltonian is, in the worst case, linear in the number of modes, and in many cases just constant. In this particular example the total number of gates per Trotter step is 33, i.e., on average 3 gates per Hamiltonian term, which is very efficient. This is due to the specific structure of this Hamiltonian, that avoids the need to apply additional local rotations.

In Fig. 2, we plot in (a) and (c) the average number of excitations for mode $b_{2\downarrow}$ (dashed, blue line) and $b_{3\uparrow}$ (solid, red line) for different parameters, showing the good convergence of the Trotter method. In (a) and (c), the lines are obtained with exact diagonalization and the dots with Trotter expansion. For additional figures with a larger number of Trotter steps, see [35]. In (b) and (c) we include the fidelity $|\langle \psi(t_F)|\psi(t_F)_T\rangle|^2$ as a function of the number of Trotter steps n_T, where $|\psi(t)\rangle$ is the state evolved with exact diagonalization, and $|\psi(t)_T\rangle$ is the Trotter-evolved
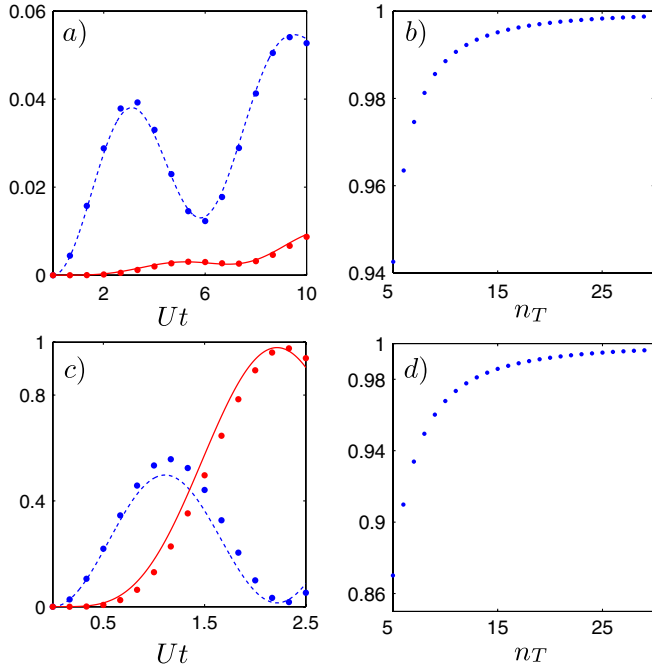
FIG. 2 (color online).　(a) $\langle b_{2\downarrow}^{\dagger} b_{2\downarrow} \rangle(t)$ (dashed, blue line), and $\langle b_{3\uparrow}^{\dagger} b_{3\uparrow} \rangle(t)$ (solid, red line) as a function of Ut, for a number of Trotter steps $n_T = 15$, and (b) fidelity $|\langle \psi(t_F) | \psi(t_F)_T \rangle|^2$ as a function of n_T, for $Ut_F = 10$, where $|\psi(t)\rangle$ is the state evolved with exact diagonalization, and $|\psi(t)_T\rangle$ is the Trotter-evolved state, for $|\psi(0)\rangle = |\psi_T(0)\rangle = b_{1\uparrow}^{\dagger} b_{1\downarrow}^{\dagger} |0\rangle$, for $|w|/U = 0.1$. (c) $\langle b_{2\downarrow}^{\dagger} b_{2\downarrow} \rangle(t)$ (dashed, blue line), and $\langle b_{3\uparrow}^{\dagger} b_{3\uparrow} \rangle(t)$ (solid, red line), for $n_T = 15$, and (d) fidelity $|\langle \psi(t_F) | \psi(t_F)_T \rangle|^2$, for $Ut_F = 2.5$, where $|\psi(t)\rangle$ is the state evolved with exact diagonalization, and $|\psi(t)_T\rangle$ is the Trotter-evolved state, for $|\psi(0)\rangle = |\psi_T(0)\rangle = b_{1\uparrow}^{\dagger} b_{1\downarrow}^{\dagger} |0\rangle$, for $|w|/U = 4$. In (a) and (c), the lines are obtained with exact diagonalization and the dots with Trotter expansion.

state, for $|\psi(0)\rangle = |\psi_T(0)\rangle = b_{1\uparrow}^{\dagger} b_{1\downarrow}^{\dagger} |0\rangle$, and for different parameters. Notice that the fidelity of the Trotter expansion goes to 1 with the number of Trotter steps n_T, and for $n_T = 10$ it is 0.99 (b) or 0.97 (d).

With current technology, more than 100 gates have been realized in a single experiment [39]. Indeed, without error correction, one would expect the realization of more than 1000 gates in the near future [40]. This will allow, for $n_T = 10$ Trotter steps, the implementation of hundreds of gates per step, giving us the possibility to simulate a wide variety of fermionic models. In a possible experiment, one could consider, e.g., strings of Ca^+ ions controlled with lasers. The spin degrees of freedom can be encoded in long-lived electronic states of the ions [5,6,12,14,19,32,39]. Optimal state initialization via optical pumping and high-fidelity detection through resonance fluorescence can be easily performed.

In conclusion, we have introduced a method for simulating efficiently, i.e., with polynomial resources, many-body fermionic lattice models in an ion string. These results may

be relevant for quantum simulations of condensed-matter systems or high-energy physics in nonperturbative regimes.

[1] R. P. Feynman, Int. J. Theor. Phys. **21**, 467 (1982).
[2] S. Lloyd, Science **273**, 1073 (1996).
[3] E. Jané, G. Vidal, W. Dür, P. Zoller, and J. I. Cirac, Quantum Inf. Comput. **3**, 15 (2003).
[4] D. Porras and J. I. Cirac, Phys. Rev. Lett. **92**, 207901 (2004).
[5] A. Friedenauer, H. Schmitz, J. T. Glueckert, D. Porras, and T. Schätz, Nature Phys. **4**, 757 (2008).
[6] K. Kim, M.-S. Chang, S. Korenblit, R. Islam, E. E. Edwards, J. K. Freericks, G.-D. Lin, L.-M. Duan, and C. Monroe, Nature (London) **465**, 590 (2010).
[7] M. Greiner, O. Mandel, T. Esslinger, T. W. Hänsch, and I. Bloch, Nature (London) **415**, 39 (2002).
[8] B. P. Lanyon, J. D. Whitfield, G. G. Gillet, M. E. Goggin, M. P. Almeida, I. Kassal, J. D. Biamonte, M. Mohseni, B. J. Powell, M. Barbieri, A. Aspuru-Guzik, and A. White, Nature Chem. **2**, 106 (2010).
[9] J. C. F. Matthews, K. Poulios, J. D. A. Meinecke, A. Politi, A. Peruzzo, N. Ismail, K. Wörhoff, M. G. Thompson, J. L. O'Brien, arXiv:1106.1166.
[10] H. Weimer, M. Müller, I. Lesanovsky, P. Zoller, and H. P. Büchler, Nature Phys. **6**, 382 (2010).
[11] L. Lamata, J. León, T. Schätz, and E. Solano, Phys. Rev. Lett. **98**, 253005 (2007).
[12] R. Gerritsma, G. Kirchmair, F. Zähringer, E. Solano, R. Blatt, and C. F. Roos, Nature (London) **463**, 68 (2010).
[13] J. Casanova, J. J. García-Ripoll, R. Gerritsma, C. F. Roos, and E. Solano, Phys. Rev. A **82**, 020101 (2010).
[14] R. Gerritsma, B. P. Lanyon, G. Kirchmair, F. Zähringer, C. Hempel, J. Casanova, J. J. García-Ripoll, E. Solano, R. Blatt, and C. F. Roos, Phys. Rev. Lett. **106**, 060503 (2011).
[15] J. Casanova, C. Sabín, J. León, I. L. Egusquiza, R. Gerritsma, C. F. Roos, J. J. García-Ripoll, and E. Solano, Phys. Rev. X **1**, 021018 (2011).
[16] L. Lamata, J. Casanova, R. Gerritsma, C. F. Roos, J. J. García-Ripoll, and E. Solano, New J. Phys. **13**, 095003 (2011).
[17] J. Casanova, L. Lamata, I. L. Egusquiza, R. Gerritsma, C. F. Roos, J. J. García-Ripoll, and E. Solano, Phys. Rev. Lett. **107**, 260501 (2011).
[18] S. P. Jordan, K. S. M. Lee, and J. Preskill, arXiv:1111.3633.
[19] J. Welzel, A. Bautista-Salvador, C. Abarbanel, V. Wineman-Fisher, C. Wunderlich, R. Folman, and F. Schmidt-Kaler, Eur. Phys. J. D **65**, 285 (2011).
[20] M. Johanning, A. F. Varón, and C. Wunderlich, J. Phys. B **42**, 154009 (2009).
[21] D. S. Abrams and S. Lloyd, Phys. Rev. Lett. **79**, 2586 (1997).

[22] M. Troyer and U.-J. Wiese, Phys. Rev. Lett. **94**, 170201 (2005).

[23] E. Y. Loh, Jr, J. E. Gubernatis, R. T. Scalettar, S. R. White, D. J. Scalapino, and R. L. Sugar, Phys. Rev. B **41**, 9301 (1990).

[24] A. C. Hewson, *The Kondo Problem to Heavy Fermions* (Cambridge University Press, Cambridge, England, 1997).

[25] R. C. Albers, N. E. Christensen, and A. Svane, J. Phys. Condens. Matter **21**, 343201 (2009).

[26] G. D. Mahan, *Many Particle Physics* (Springer, New York, 2000).

[27] F. Schwabl, *Advanced Quantum Mechanics* (Springer, New York, 2005).

[28] P. Jordan and E. Wigner, Z. Phys. **47**, 631 (1928).

[29] M. A. Nielsen and I. L. Chuang, *Quantum Computation and Quantum Information* (Cambridge University Press, Cambridge, England, 2000).

[30] D. W. Berry, G. Ahokas, R. Cleve, and Barry C. Sanders, Commun. Math. Phys. **270**, 359 (2006).

[31] M. Müller, K. Hammerer, Y. L. Zhou, C. F. Roos, and P. Zoller, New J. Phys. **13**, 085007 (2011).

[32] J. T. Barreiro, M. Müller, P. Schindler, D. Nigg, T. Monz, M. Chwalla, M. Hennrich, C. F. Roos, P. Zoller, and R. Blatt, Nature (London) **470**, 486 (2011).

[33] F. Verstraete and J. I. Cirac, J. Stat. Mech. (2005) P09012.

[34] E. Farhi, J. Goldstone, S. Gutmann, and M. Sipser, arXiv:quant-ph/0001106.

[35] See Supplemental Material at http://link.aps.org/supplemental/10.1103/PhysRevLett.108.190502 for several examples of our method and an analysis of the Trotter errors.

[36] J. Kondo, Prog. Theor. Phys. **32**, 37 (1964).

[37] D. Leibfried, R. Blatt, C. Monroe, and D. Wineland, Rev. Mod. Phys. **75**, 281 (2003).

[38] G. L. Goodvin, A. S. Mishchenko, and M. Berciu, Phys. Rev. Lett. **107**, 076403 (2011).

[39] B. P. Lanyon, C. Hempel, D. Nigg, M. Müller, R. Gerritsma, F. Zähringer, P. Schindler, J. T. Barreiro, M. Rambach, G. Kirchmair, M. Hennrich, P. Zoller, R. Blatt, and C. F. Roos, Science **334**, 57 (2011).

[40] Rainer Blatt (private communication).